JOURNAL OF MATERIALS SCIENCE 40 (2005) 5925–5932

Mesoscopic fabric models using a discrete mass-spring approach: Yarn-yarn interactions analysis

BILEL BEN BOUBAKER*, BERNARD HAUSSY
ESEO. 4, rue Merlet de la Boulaye, 49009 Angers Cedex 01, BP 926, France
E-mail: Bilel.ben_boubaker@eseo.fr
E-mail: Bernard.haussy@eseo.fr

JEAN-FRANCOIS GANGHOFFER
LEMTA, UMR 7563, ENSEM. 2, Avenue de la Forêt de Haye, B.P. 160, 54504 VANDOEUVRE Cedex, France
E-mail: jfgangho@ensem.inpl-nancy.fr

A meso/macro discrete model of fabric has been developed, accounting for yarn-yarn interactions occurring at the crossing points. The fabric yarns, described initially by a Fourier series development, are discretized into elastic straight bars represented by stretching springs and connected at frictionless hinges by rotational springs. The motion of each node is described by a lateral displacement and a rotation. The compressibility of both yarns is expressed as a kinematic relationship, considering frictionless motions of the yarns. The expression of the reaction force exerted by the transverse yarns at the contact points is then assessed, from which the work of the reaction forces is established. The equilibrium shape of the yarn is obtained as the minimum of its total potential energy, accounting for the work of the reaction forces due to the transverse yarns. Simulations of a traction curve of a single yarn are performed, that evidence the effect of the yarn interactions and the main deformation mechanisms.

1. Introduction

The analysis of the deformations and shape forming of woven structures such as textiles is nowadays an important scientific and technological topic, due to the wide range of applications of these structures : mention e.g. composites with a woven reinforcement used in aerospace industry for their gain of weight; clothes industry, or geotextiles. Three imbricated scales can be identified: the microscopic scale (scale of the yarn), the macroscopic scale of the woven structure, and an intermediate scale of a few intertwined yarns, that defines the unit cell reproducing the whole structure by a periodic translation, called the mesoscopic scale. The organisation of the yarns within the unit cell, (that defines different armours, such as satin, serge) and the interactions between yarns (contact, friction) play an important role in favouring the shape forming of the initially flat structure. It is therefore important to develop reliable and accurate micromechanical models, in order to predict the 3D deformation of woven structures during real forming processes. These models can then further be used at the next scale (the macro scale) and implemented in FE codes [1–7]; this description can be refined, using the so-called meso-macro models that account for the nonlinearities due to the change of undulations of the yarns [8, 9]. A synthetic view of the modelling of woven structures is given in [10].

A discrete model of fabric has been developed [11], relying on a topological description of the yarns as an undulated beam modelled by analogical spring elements, in connection with a given kinematics of the analogical elements (extensional, flexional and torsional springs). The analogical modelling strategy of woven structures has been developed at both the macroscopic scale (the unit cell is endowed by extension, shear, torsion and bending deformation modes that mimic the kinematics of a piece of fabric at the structural scale) and the mesoscopic scale: the basic difference is that the mesoscopic model explicitly considers the yarn shape, thus account for the change of yarn undulations that are responsible for the geometrical nonlinearities observed at the macroscopic level.

The discrete approaches presented in this work bears some resemblance with the work by Provot [12], who models the tissue by a set of punctual masses connected with extensional, flexional and shear-like springs;

*Author to whom all correspondence should be addressed.

0022-2461 © 2005 Springer Science + Business Media, Inc.
DOI: 10.1007/s10853-005-5056-z

however, the model elaborated by this author does only consider the in-plane deformation of the pattern, and thus excludes the displacements of the nodes outside the initial plane of the tissue. The present model is intended to give a generalized description of the yarns motion and interactions.

As the woven structure becomes stretched, the interaction between both sets of yarns (warp and weft) is increased, and one should expect that the ability of the tissue to deform shall be accordingly modified: it is intuitively clear that the yarn mobility is reduced at the contact zone between both yarns, specially in terms of rotation. This in turn affect the shape forming capacity of woven structures at the macroscopic scale. Few works in the literature have been devoted to the analysis of the contact interactions between the yarns, including yarn interactions and compressibility, notwithstanding 3D finite element analysis within a context of contact mechanics (see e.g. [13]). The goal of the developed approach of the interactions between yarns is to incorporate the effect of the contact in a manner compatible with the represented discrete model, at a mesoscopic scale, thus without considering the three-dimensional picture inherent to a microscopic view of the yarns contact problem.

2. Discrete model description: Consideration of the contact between warp and weft

One considers in the sequel the plane motion of a single yarn (the warp) subjected to traction at its extremities and to the punctual contact reactions exerted by the transverse yarns (the weft), Fig. 1. Although this situation is somewhat artificial (since we isolate mentally the yarn from the trellis), it gives a first insight into the interaction effect between both sets of yarns. The discretized yarn consists of a set of punctual masses mutually connected by extensional rigidities $C_{ei} = \mathrm{EA}/\Delta$; each node is given a rigidity in flexion $C_{bi} = \mathrm{EI}/\Delta$ (Δ is the curvilinear distance between two consecutive nodes), Fig. 1.

The kinematics of the yarn is described on Fig. 1, and consists of the vertical displacements W_i and the rotations ψ_i (the rotation axis being orthogonal to the plane of Fig. 1) of the connecting nodes. In the sequel, the contact forces exerted by each transverse yarn (marked with a cross on Fig. 1) are first expressed, involving the Timoshenko beam theory [14].

3. Determination of the warp and weft interactions

In this section, we first study the yarn-yarn interactions within the woven structure, submitted to an external biaxial loading. We will first express the reaction force occurring at the interlacing points, in terms of the mechanical and geometrical yarns parameters, and the traction loads P_{wa} and P_{we} applied in the x and y direction respectively.

At equilibrium, the deformed shapes of the fabric yarns are assumed to be periodic and expressed as the following Fourier series:

- $$w_{we}^{j}(y) = \sum_{n=1}^{N_{wa}} a_{n,j}^{we} \sin\left((j-1)\pi + n\frac{\pi y}{L_{we}}\right),$$ for a weft yarn of index j
- $$w_{wa}^{k}(x) = \sum_{n=1}^{N_{we}} a_{n,k}^{wa} \sin\left((k-1)\pi + n\frac{\pi x}{L_{wa}}\right),$$ for a warp yarn of index k

where L_{wa} (resp. L_{we}) is the projected length of the warp (resp. the weft) yarns on the x-axis (resp. y-axis), and the $(a_n^{wa})_{n\in[1,N_{we}]}$, $(a_n^{we})_{n\in[1,N_{wa}]}$ are the Fourier series coefficients.

In order to establish the expression of the reaction force exerted at the yarn-yarn contact points, we analyze the mechanical behavior of the system Ω_{we} consisting of the N_{we} weft yarns: in this case, the sub system Ω_{wa} consisting of the set of warp (N_{wa} yarns) is

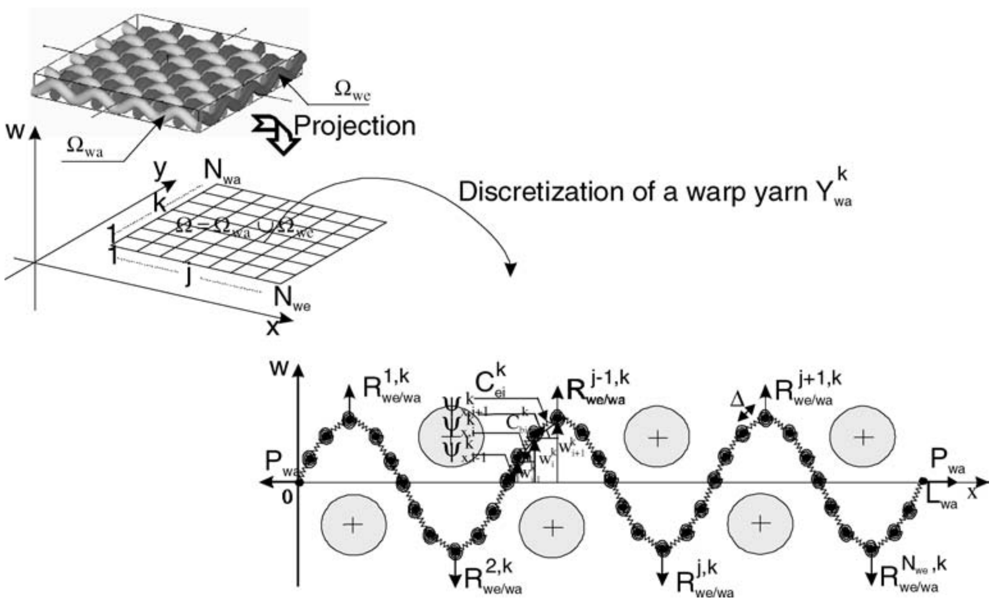

Figure 1 Discrete model of the yarn isolated from the trellis.

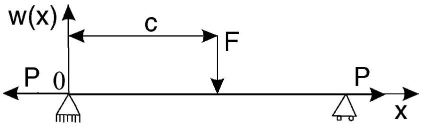

Figure 2 Elastic beam subjected to lateral and axial loads.

considered as an external system; accordingly, the contact forces exerted on the weft yarns are considered as external forces for Ω_{we}. Using the Timoshenko's beam theory, in the case of an elastic beam subjected to an axial load P and a lateral force F exerted at a point of abscissa c (Fig. 2), the equilibrium shape of the elastic beam is given by the Fourier series

$$w(x) = \frac{2FL^3}{\pi^4 \mathrm{EI}} \sum_{k=1}^{N} \frac{1}{k^2\left(k^2 + \frac{P}{P_{\mathrm{cr}}}\right)} \sin\left(\frac{k\pi c}{L}\right) \times \sin\left(\frac{k\pi x}{L}\right) \quad (1)$$

with $P_{\mathrm{cr}} = \frac{\pi^2 \mathrm{EI}}{L^2}$, the beam critical compressive load

L the projected beam length and EI the beam bending rigidity

Using the superposition principle, the equilibrium shape associated to a weft yarn, treated as an elastic beam subjected to an axial load and periodic lateral forces (Fig. 3), is defined by the Fourier series coefficients, viz

$$a_{n,j}^{\mathrm{we}} = \frac{2R_{\mathrm{wa/we}} L_{\mathrm{we}}^3}{\pi^4 \mathrm{EI}_{\mathrm{we}}} \sum_{m=1}^{N_{\mathrm{wa}}/2} \frac{1}{n^2(n^2 + \alpha_{\mathrm{we}})} \times \left[\sin\left(\frac{n\pi}{N_{\mathrm{wa}}}\left(2m - \frac{3}{2}\right)\right) - \sin\left(\left(2m - \frac{1}{2}\right)\frac{n\pi}{N_{\mathrm{wa}}}\right)\right] \quad \forall n \in [1,\ N_{\mathrm{wa}}] \quad (2)$$

with $\alpha_{\mathrm{we}} = \frac{P_{\mathrm{we}}}{P_{\mathrm{cr}}^{\mathrm{we}}}$ and $P_{\mathrm{cr}}^{\mathrm{we}} = \frac{\pi^2 \mathrm{EI}_{\mathrm{we}}}{L_{\mathrm{we}}^2}$.

We then deduce the deformed shape of a weft yarn of index j, in terms of the reaction force $R_{\mathrm{wa/we}}$, as

$$w_{\mathrm{we}}^{j}(y) = \frac{2R_{\mathrm{wa/we}} L_{\mathrm{we}}^3}{\pi^4 \mathrm{EI}_{\mathrm{we}}} \sum_{n=1}^{N_{\mathrm{wa}}} \sum_{m=1}^{N_{\mathrm{wa}}/2} \frac{1}{n^2(n^2 + \alpha_{\mathrm{we}})} \times \left[\sin\left(\frac{n\pi}{N_{\mathrm{wa}}}\left(2m - \frac{3}{2}\right)\right) - \sin\left(\left(2m - \frac{1}{2}\right)\frac{n\pi}{N_{\mathrm{wa}}}\right)\right] \times \sin\left((j-1)\pi + \frac{n\pi y}{L_{\mathrm{we}}}\right) \quad (3)$$

This result shows that the deformed shape of the weft yarns within a woven structure at equilibrium is known from the values of the applied traction P_{we} (trough the ratio α_{we}) and the yarn-yarn contact forces. We note $\tilde{w}_{\mathrm{we}} = A_{\mathrm{we}}$ the amplitude of the weft yarns within the woven structure, defined at the contact points abscissas (Fig. 3) by

$$\tilde{w}_{\mathrm{we}} = \left|w_{\mathrm{we}}^{j}(c_j)\right| \quad (4)$$

At the interlacing points, the new double sum of the Equation 3 simplifies as

$$\left|\sum\sum\right| = \frac{1}{N_{\mathrm{wa}}\left(N_{\mathrm{wa}}^2 + \alpha_{\mathrm{we}}\right)} \quad \text{for} \quad y = c_k \quad \forall k \in [1,\ N_{\mathrm{wa}}] \quad (5)$$

We deduce then, from Equations 3–5, the expression of the reaction forces that exert the transverse yarns on the weft yarns at the interlacing points, accordingly to the amplitude undulations $\tilde{w}_{\mathrm{we}} = A_{\mathrm{we}}$, thus we have

$$\begin{aligned} \forall y = c_k, \quad |w_{\mathrm{we}}(y)| &= \tilde{w}_{\mathrm{we}} \\ &= \frac{2R_{\mathrm{wa/we}}}{\pi^4 \mathrm{EI}_{\mathrm{we}}} \frac{L_{\mathrm{we}}^3}{N_{\mathrm{wa}}\left(N_{\mathrm{wa}}^2 + \alpha_{\mathrm{we}}\right)} \Leftrightarrow R_{\mathrm{wa/we}} \\ &= \frac{\pi^4}{2} \frac{\mathrm{EI}_{\mathrm{we}}}{\left(L_p^{\mathrm{we}}\right)^3}\left(1 + \frac{\alpha_{\mathrm{we}}}{N_{\mathrm{wa}}^2}\right)\tilde{w}_{\mathrm{we}} \end{aligned} \quad (6)$$

In the case of only one reaction force (N_{wa}=1), applied at the middle of the yarn, we find a result identical to that of Timoshenko [13], such as

$$F = \frac{\pi^4}{2} \frac{\mathrm{EI}}{L^3}(1 + \alpha)\,\tilde{w} \quad (7)$$

This general framework shall be involved in the sequel to analyse the behaviour of a single yarn, accounting for the interactions of the transverse yarns.

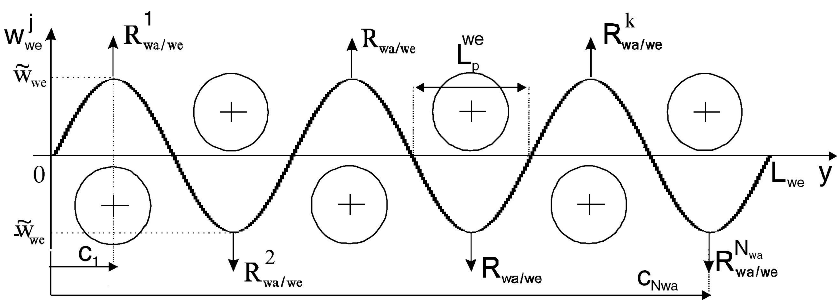

Figure 3 Distributed contact forces exerted on a weft yarn of index j.

4. Effect of the yarn-yarn interactions on the fabric extension behaviour: case of a single yarn

In this paragraph, we analyse the effect of the interaction between the weft and the warp yarns for a single warp yarn loaded by a traction force, and subjected to its own weight. For this purpose, we consider two different cases:

(i) Case of a warp yarn within a woven structure, submitted to the interactions of the transverse yarns;
(ii) Case of an initially deformed yarn, being extracted from the woven structure (thus free of contact with other yarns), having the same mechanical and geometrical properties.

In both cases, the yarn shapes are assumed to be periodic, their equilibrium shapes being expressed as Fourier series development limited to the first $N_{\rm we}$ harmonics, viz

$$w_{\rm wa}(x) = \sum_{n=1}^{N_{\rm we}} a_n^{\rm wa} \sin\left(n\pi \frac{x}{L_{\rm wa}}\right) \quad \text{(case of a warp yarn of index } k = 1) \tag{8}$$

with $L_{\rm wa}$ the projected length of the yarn on the x-axis and $N_{\rm we}$ the number of half-periods of undulation. In the case of a warp yarn within the woven structure, it is the number of transverse yarns contacts.

Under the traction loads $P_{\rm wa}$, the equilibrium state (with or without lateral contacts), is obtained as the minimum of the total potential energy of the deformed yarns. In each case, the expression of the total potential energy is established as a function of the kinematical yarn parameters (the displacements u_i, w_i and the rotations ψ_i of the yarn's nodes). The work of the reaction force occurring at the interlacing points is first expressed.

4.1. Yarn-yarn interaction model account for yarn compressibility

Considering perfect contact conditions (absence of sliding between the yarns, not to say case of a blocked structure), the continuity condition of the displacement at the contact points expresses as the following relationship between the vertical displacements of the summits of the undulations of the yarns (best illustrated on Fig. 4)

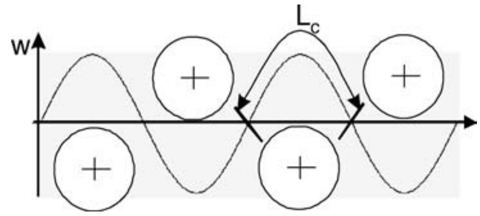

Figure 5 Definition of a yarn portion length (under half-period).

$$\begin{aligned} \delta_t^{\rm wa} &= \delta_t^{\rm we} \Rightarrow \\ {\rm w}_{\rm s-we} &= \left({\rm w}_{\rm so-we} + \delta_{\rm comp}^{\rm we}\right) + {\rm w}_{\rm s-wa} - \left({\rm w}_{\rm so-wa} - \delta_{\rm comp}^{\rm wa}\right) \\ &= {\rm w}_{\rm s-wa} - {\rm w}_{\rm so-wa} + {\rm w}_{\rm so-we} + \delta_{\rm comp}^{\rm we} + \delta_{\rm comp}^{\rm wa} \end{aligned} \tag{9}$$

in which $\delta_{\rm comp}^{\rm we}$ and $\delta_{\rm comp}^{\rm wa}$ are new kinematic variables, that respectively denote the vertical displacement of the warp and weft under compression (Fig. 4).

The deformation under compression of a warp, $\delta_{\rm comp}^{\rm wa}$, varies vs. the contact force exerted by the transverse weft according to the following phenomenological law [15–17], that can be easily inverted:

$$\delta_{\rm comp}^{\rm wa} = C_1\left(1 - e^{-K_1|R_{\rm we/wa}|/L_{\rm c}^{\rm wa}}\right) \Leftrightarrow |R_{\rm we/wa}| = -\frac{L_{\rm c}^{\rm wa}}{K_1}\ln\left(1 - \frac{\delta_{\rm comp}^{\rm wa}}{C_1}\right) \tag{10}$$

with C_1, K_1 the two Kawabata parameters for the warp and $L_{\rm c}$ the curvilinear length of a yarn portion defined within a half-period as shown in Fig. 5. In the same way, the deformation under compression of a weft, $\delta_{\rm comp}^{\rm tr}$, varies vs. the contact force exerted by the warp according to

$$\delta_{\rm comp}^{\rm we} = C_2\left(1 - e^{-K_2|R_{\rm wa/we}|/L_{\rm c}^{\rm we}}\right) \Leftrightarrow |R_{\rm wa/we}| = -\frac{L_{\rm c}^{\rm we}}{K_2}\ln\left(1 - \frac{\delta_{\rm comp}^{\rm we}}{C_2}\right) \tag{11}$$

with C_2, K_2 the two Kawabata parameters of the weft. Note that this way of accounting of the yarn compressibility is global with regard to the yarn geometry, since for instance the real shape of the yarn cross-section is

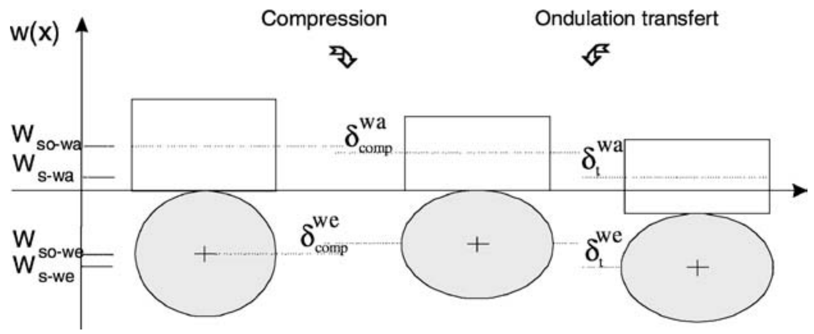

Figure 4 Compression and undulation transfer between yarns.

not considered (the 3D representation in Fig. 4a supports the explanation of what really happens at the microscopic scale, whereas the modeling only account for the mean line interactions of the beams that represents the yarns).

According to the action/reaction principle valid at the contact points, viz $|R_{\mathrm{we/wa}}| = |R_{\mathrm{wa/we}}|$, the compression displacements of both yarns are further related by the following relationship

$$\delta_{\mathrm{comp}}^{\mathrm{we}} = C_2\left[1-\left(1-\frac{\delta_{\mathrm{comp}}^{\mathrm{wa}}}{C_1}\right)^{\frac{K_2}{K_1}\frac{L_c^{\mathrm{wa}}}{L_c^{\mathrm{we}}}}\right] \quad (12)$$

Equations 9 and 12 then lead to

$$w_{\mathrm{s-tr}} = \mathrm{w}_{\mathrm{s-wa}} - \mathrm{w}_{\mathrm{so-wa}} + \mathrm{w}_{\mathrm{so-we}} + C_2 \times\left[1-\left(1-\frac{\delta_{\mathrm{comp}}^{\mathrm{wa}}}{C_1}\right)^{\frac{K_2}{K_1}\frac{L_c^{wa}}{L_c^{\mathrm{we}}}}\right] + \delta_{\mathrm{comp}}^{\mathrm{wa}} \quad (13)$$

From the relation 6, which expresses the reaction force exerted by the warp on the weft (constrained by the lateral reaction forces only: P_{we}=0), and the relation 13, we deduce the reaction force (with $\alpha_{\mathrm{we}} = \frac{P_{\mathrm{we}}}{P_{\mathrm{cr}}^{\mathrm{we}}} = 0$ in this case)

$$R_{\mathrm{wa/we}} = \frac{\pi^4}{2}\frac{(\mathrm{EI})_{\mathrm{we}}}{\left(L_{\mathrm{p}}^{\mathrm{we}}\right)^3}\mathrm{w}_{\mathrm{s-we}} = \frac{\pi^4}{2}\frac{(\mathrm{EI})_{\mathrm{we}}}{\left(L_p^{\mathrm{we}}\right)^3}\left[(\mathrm{w}_{\mathrm{so-we}}-\mathrm{w}_{\mathrm{so-wa}})+\mathrm{w}_{\mathrm{s-wa}}+C_2\left[1-\left(1-\frac{\delta_{\mathrm{comp}}^{\mathrm{wa}}}{C_1}\right)^{\frac{K_2}{K_1}\frac{L_c^{\mathrm{wa}}}{L_c^{\mathrm{we}}}}\right]+\delta_{\mathrm{comp}}^{\mathrm{wa}}\right] \quad (14)$$

Using now the action-reaction principle, the reaction force exerted by the weft on the warp at the crossing points is given by

$$R_{\mathrm{we/wa}} = -R_{\mathrm{wa/we}} = -\frac{\pi^4}{2}\frac{(\mathrm{EI})_{\mathrm{we}}}{\left(L_p^{\mathrm{we}}\right)^3}\left[(\mathrm{w}_{\mathrm{so-we}}-\mathrm{w}_{\mathrm{so-wa}})+\mathrm{w}_{\mathrm{s-wa}}+C_2\left[1-\left(1-\frac{\delta_{\mathrm{comp}}^{\mathrm{wa}}}{C_1}\right)^{\frac{K_2}{K_1}\frac{L_c^{\mathrm{wa}}}{L_c^{\mathrm{we}}}}\right]+\delta_{\mathrm{comp}}^{\mathrm{wa}}\right] \quad (15)$$

Therefore, the work of the reaction force exerted by the weft on the warp at a crossing node having index j is given by

$$\begin{aligned}
\mathrm{W}_{R_{\mathrm{we/wa}}^j} &= \int_{w_{\mathrm{so-wa}}^j}^{w_{\mathrm{s-wa}}^j} R_{\mathrm{we/wa}}\,dw \\
&= \int_{w_{\mathrm{so-wa}}^j}^{w_{\mathrm{s-wa}}^j} -\frac{\pi^4}{2}\frac{(\mathrm{EI})_{\mathrm{we}}}{\left(L_p^{\mathrm{we}}\right)^3}\left[\left(w_{\mathrm{so-we}}^j - w_{\mathrm{so-wa}}^j\right) + C_2\left[1-\left(1-\frac{\delta_{\mathrm{comp}}^{\mathrm{wa}}}{C_1}\right)^{\frac{K_2}{K_1}\frac{L_c^{\mathrm{wa}}}{L_c^{\mathrm{we}}}}\right] + \delta_{\mathrm{comp}}^{\mathrm{wa}} + w\right]dw \\
&= -\frac{\pi^4}{2}\frac{(\mathrm{EI})_{\mathrm{we}}}{\left(L_p^{\mathrm{wa}}\right)^3}\left[\begin{array}{l}\left(\left(w_{\mathrm{so-we}}^j - w_{\mathrm{so-wa}}^j + C_2\left[1-\left(1-\frac{\delta_{\mathrm{comp}}^{\mathrm{wa}}}{C_1}\right)^{\frac{K_2}{K_1}\frac{L_c^{\mathrm{wa}}}{L_c^{\mathrm{we}}}}\right] + \delta_{\mathrm{comp}}^{\mathrm{wa}}\right)w_{\mathrm{s-wa}}^j + \frac{1}{2}w_{\mathrm{s-wa}}^{j2}\right) \\ -\left(\left(w_{\mathrm{so-we}}^j - w_{\mathrm{so-wa}}^j + C_2\left[1-\left(1-\frac{\delta_{\mathrm{comp}}^{\mathrm{wa}}}{C_1}\right)^{\frac{K_2}{K_1}\frac{L_c^{\mathrm{wa}}}{L_c^{\mathrm{we}}}}\right] + \delta_{\mathrm{comp}}^{\mathrm{wa}}\right)w_{\mathrm{so-wa}}^j + \frac{1}{2}{w_{\mathrm{so-wa}}^j}^2\right)\end{array}\right]
\end{aligned} \quad (16)$$

This work further enters in the determination of the total work of the applied external forces (gravity forces, traction loads), viz

$$W_{\mathrm{ext}} = W_{\mathrm{tr}} + W_{\mathrm{gr}} + W_{\mathrm{reaction}} \quad (17)$$

where W_{tr} refers to the work of the traction loads P_{wa} and $\mathrm{W_{gr}}$ corresponds to the work of the gravity forces.

The global displacement Δu_{wa} experienced by the end nodes of the warp is decomposed into the sum of a flexional contribution Δu_{wa}^f (yarn end-displacement due to the undulation variation) and an extensional contribution $\Delta u_{\mathrm{wa}}^{\mathrm{ex}}$ (yarn end-displacement due to the stretching of the yarn), viz

$$\Delta u_{\mathrm{wa}} = \Delta u_{\mathrm{wa}}^f + \Delta u_{\mathrm{wa}}^{;\mathrm{ex}}$$

$$\text{with} \quad \begin{cases}\Delta u_{\mathrm{wa}}^f = \sum_{i=1}^{N_d}\Delta(\cos(\psi_{x,i}) - \cos(\psi_{x,\mathrm{oi}})) \\ \Delta u_{\mathrm{wa}}^{\mathrm{ex}} = u_{N_d+1}\end{cases} \quad (18)$$

thus

$$\Delta u_{\mathrm{wa}} = \sum_{i=1}^{N_d}\Delta(\cos(\psi_{x,i}) - \cos(\psi_{x,\mathrm{oi}})) + u_{N_d+1} \quad (19)$$

For small rotations, the global displacement can be written as

$$\Delta u_{\mathrm{wa}} \approx \sum_{i=1}^{N_d}\frac{\Delta}{2}((\psi_{x,i})^2 - (\psi_{x,\mathrm{oi}})^2) + u_{N_d+1} \quad (20)$$

The work of the applied load P_{wa} is accordingly

$$W_{\mathrm{traction}} = P_{\mathrm{wa}}\left(\sum_{i=1}^{N_d}\frac{\Delta}{2}\left((\psi_{x,i}^k)^2 - (\psi_{x,\mathrm{oi}}^k)^2\right) + u_{N_d+1}^k\right) \quad (21)$$

Summarizing previous results, the expression of the external work W_{ext} becomes

$$W_{\mathrm{ext}} = -\frac{\pi^4}{2}\frac{(\mathrm{EI})_{\mathrm{we}}}{(L_p^{\mathrm{wa}})^3}\begin{bmatrix} \left(\left(w^j_{\mathrm{so-we}} - w^j_{\mathrm{so-wa}} + C_2\left[1-\left(1-\frac{\delta^{\mathrm{wa}}_{\mathrm{comp}}}{C_1}\right)^{\frac{K_2}{K_1}\frac{L_c^{\mathrm{wa}}}{L_c^{\mathrm{we}}}}\right] + \delta^{\mathrm{wa}}_{\mathrm{comp}}\right) w^j_{\mathrm{s-wa}} + \frac{1}{2} w^{j2}_{\mathrm{s-wa}}\right) \\ -\left(\left(w^j_{\mathrm{so-we}} - w^j_{\mathrm{so-wa}} + C_2\left[1-\left(1-\frac{\delta^{\mathrm{wa}}_{\mathrm{comp}}}{C_1}\right)^{\frac{K_2}{K_1}\frac{L_c^{\mathrm{wa}}}{L_c^{\mathrm{we}}}}\right] + \delta^{\mathrm{wa}}_{\mathrm{comp}}\right) w^j_{\mathrm{so-wa}} + \frac{1}{2} w^{j2}_{\mathrm{so-wa}}\right) \end{bmatrix}$$
$$+P_{\mathrm{wa}}\left(\sum_{i=1}^{N_d}\frac{\Delta}{2}\left(\psi_i^2 - \psi_{\mathrm{oi}}^2\right) + u_{n+1}\right) - \sum_{i=1}^{N_d-1} m_i g\left(w_i - w_i^o\right) \quad (22)$$

with N_d the number of discrete elements; the index 0 refers to the initial value corresponding to a kinematical variable at the initial state.

The total potential energy V is then obtained as the difference between the internal deformation energy U (due to the flexion, extension and the compression of the yarn of total length $L_s^{\mathrm{wa}} = N_{\mathrm{we}} L_{\mathrm{c}}^{\mathrm{wa}}$), viz

$$U = U_{\mathrm{F}} + U_{\mathrm{ex}} + U_{\mathrm{comp}} = \sum_{i=1}^{N_d-1}\frac{1}{2}C_{\mathrm{bi}}\left(\psi_{x,i+1} - \psi_{x,i}\right)^2 + \sum_{i=1}^{N_d}\frac{1}{2}C_{\mathrm{ei}}\left(u_{i+1} - u_i\right)^2 + \frac{L_{\mathrm{s}}^{\mathrm{wa}}}{K_1} \times \left[\left(C_1 - \delta^{\mathrm{wa}}_{\mathrm{comp}}\right)\ln\left(1 - \frac{\delta^{\mathrm{wa}}_{\mathrm{comp}}}{C_1}\right) + \delta^{\mathrm{wa}}_{\mathrm{comp}}\right] \quad (23)$$

and the work of the external forces W_{ext}, thus leading to

$$V = \begin{pmatrix} \sum_{i=1}^{N_d-1}\frac{1}{2}C_{\mathrm{bi}}(\psi_{x,i+1} - \psi_{x,i})^2 + \sum_{i=1}^{N_d}\frac{1}{2}C_{\mathrm{ei}}\left(u_{i+1} - u_i\right)^2 + \frac{L_s^{\mathrm{wa}}}{K_1}\left[\left(C_1 - \delta^{\mathrm{wa}}_{\mathrm{comp}}\right)\ln\left(1 - \frac{\delta^{\mathrm{wa}}_{\mathrm{comp}}}{C_1}\right) + \delta^{\mathrm{wa}}_{\mathrm{comp}}\right] \\ -P_{\mathrm{wa}}\left(\sum_{i=1}^{N_d}\Delta(\cos(\psi_{x,i}) - \cos(\psi_{x,\mathrm{oi}})) + u_{N_d+1}\right) + \sum_{i=1}^{N_d-1} m_i g\left(w_i - w_{\mathrm{oi}}\right) \end{pmatrix}$$
$$+\sum_{j=1}^{N_{we}}\frac{\pi^4}{2}\frac{(\mathrm{EI})_{\mathrm{we}}}{\left(L_p^{\mathrm{we}}\right)^3}\begin{bmatrix} \left(\left(w^j_{\mathrm{so-we}} - w^j_{\mathrm{so-wa}} + C_2\left[1-\left(1-\frac{\delta^{\mathrm{wa}}_{\mathrm{comp}}}{C_1}\right)^{\frac{K_2}{K_1}\frac{L_c^{\mathrm{wa}}}{L_c^{\mathrm{we}}}}\right] + \delta^{\mathrm{wa}}_{\mathrm{comp}}\right) w^j_{\mathrm{s-wa}} + \frac{1}{2} w^{j2}_{\mathrm{s-wa}}\right) - \\ \left(\left(w^j_{\mathrm{so-we}} - w^j_{\mathrm{so-wa}} + C_2\left[1-\left(1-\frac{\delta^{\mathrm{wa}}_{\mathrm{comp}}}{C_1}\right)^{\frac{K_2}{K_1}\frac{L_c^{\mathrm{wa}}}{L_c^{\mathrm{we}}}}\right] + \delta^{\mathrm{wa}}_{\mathrm{comp}}\right) w^j_{\mathrm{so-wa}} + \frac{1}{2} w^{j2}_{\mathrm{so-wa}}\right) \end{bmatrix} \quad (24)$$

The index j, giving the order of the crossing points, is replaced in the previous expression by the global discretization index i such as

$$w^j_{\mathrm{s-ch}} = w_i \quad \text{with} \quad i = \frac{(2j-1)\,N_d}{2N_{\mathrm{we}}} \quad (25)$$

We notice that the total potential energy involves two dependent variables ψ and w with

$$\sin\psi_{x,i} = \frac{w_i - w_{i-1}}{\Delta} \quad (26)$$

The discrete displacements $(w_i)_i$ are obtained from the discretization of the continuous position $w_{\mathrm{wa}}(x) = \sum_{n=1}^{N_{\mathrm{we}}} a_n^{\mathrm{wa}} \sin(n\pi\frac{x}{L_{\mathrm{wa}}})$ according to

$$\forall\, i \in [1, N_d - 1]\ \ w_i = w_{\mathrm{wa}}(x_i) = \sum_{n=1}^{N_{\mathrm{we}}} a_n^{\mathrm{wa}} \sin\left(\frac{n\pi}{L}x_i\right) \quad \text{with} \quad x_i = \frac{iL}{N_d} \quad (27)$$

Using the relations (26) and (27), the total potential energy given by Equation 24 is expressed only in terms of the coefficients $(a_n^{\mathrm{wa}})_{n\in[1,N_{\mathrm{we}}]}$ of the Fourier series, together with the extensions $(u_2, u_3, \ldots, u_{N_d+1})$ of the nodes of the discrete warp yarn (accounting for the condition u_1=0), as

$$V = V\left(a_1^{\mathrm{wa}}, \ldots a_2^{\mathrm{wa}}, \ldots a_{N_{\mathrm{we}}}^{\mathrm{wa}}, u_2, \ldots u_i, \ldots u_{N_d+1}, \delta^{\mathrm{wa}}_{\mathrm{comp}}\right) \quad (28)$$

The yarn equilibrium shape is given by the minimization of the total potential energy with respect to the set of arguments $(a_1^{\mathrm{wa}}, \ldots a_2^{\mathrm{wa}}, \ldots a_{N_{\mathrm{we}}}^{\mathrm{wa}}, u_2, \ldots u_i, \ldots u_{N_d+1}, \delta^{\mathrm{wa}}_{\mathrm{comp}})$, i.e. by the following set of algebraic equations:

$$\frac{\partial V}{\partial a_1^{\mathrm{wa}}} = \cdots = \frac{\partial V}{\partial a_i^{\mathrm{wa}}} = \cdots = \frac{\partial V}{\partial a_{N_{\mathrm{we}}}^{\mathrm{wa}}} = 0;$$
$$\frac{\partial V}{\partial u_2} = \cdots = \frac{\partial V}{\partial u_i} = \cdots = \frac{\partial V}{\partial u_{N_d+1}} = 0$$
$$\text{and} \quad \left(\frac{\partial V}{\partial \delta^{\mathrm{wa}}_{\mathrm{comp}}}\right) = 0 \quad (29)$$

This set of equations has to be completed by the boundary condition (clamped extremity): U_1=0.

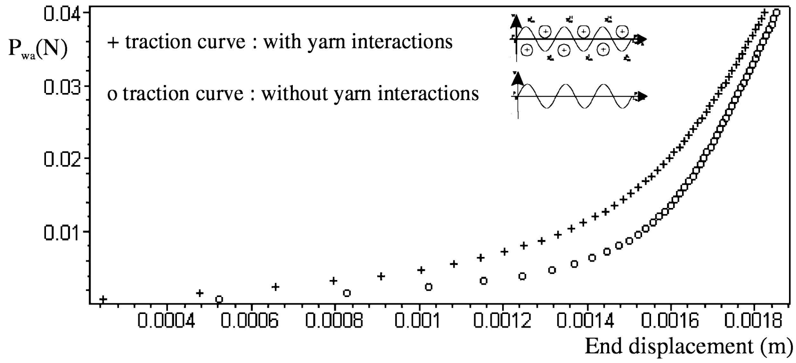

Figure 6 Unidirectional traction curve of the warp yarn. Effect of yarn-yarn interactions.

4.2. Numerical simulations

In the sequel, the developed modeling shall be exemplified by numerical simulations of the motion of one single yarn, under the simplifying assumption of incompressibility of its section. Considering carbon fibers reinforced fabric, the following input parameters are used (SNECMA, [18]): the mechanical properties of the warp and weft yarns are taken as (we neglect the compressibility of both yarns),

$$\begin{cases} \mathrm{EI_{wa}} = 1.47\mathrm{e}^{-7}\ \mathrm{N{\cdot}m^2} \\ \mathrm{EI_{we}} = 1.47\mathrm{e}^{-7}\ \mathrm{N{\cdot}m^2} \\ \mathrm{EA_{wa}} = 13.72\ \mathrm{N} \end{cases}$$

The rigidities in flexion/extension of the springs are then evaluated as

$$\begin{cases} C_b = \dfrac{\mathrm{EI_{wa}}}{\Delta} \\ C_e = \dfrac{\mathrm{EA_{wa}}}{\Delta} \end{cases}$$

The geometrical parameters of the discretization scheme are selected as:

$$\begin{cases} L_0 = 0.1\ \mathrm{m} \\ w_{\mathrm{so-wa}} = 0.5\ \mathrm{mm} \\ w_{\mathrm{so-we}} = 0.5\ \mathrm{mm} \\ N_{\mathrm{we}} = 16;\ N_d = 224 \end{cases}$$

The yarn is subjected to an increasing traction load at its extremities, and one represents the traction load vs. the yarn end-displacement (Fig. 6); the simulation without yarn interactions serves as a reference comparison case to assess the interaction effect. The mean curve of the yarn is restricted to the (x, y) plane, (Fig. 4), and both extremities of the yarn keep aligned with the direction of traction. The extension of the yarn is here defined as the displacement of the end node of the undulated beam. The simulation reproduces in a satisfactory manner the essential trend of the measured *J*-shape unidirectional traction curve.

The traction curves evidences two different deformation mechanisms: the first mechanism is the undulation variation, corresponding to the first part of the response (in fact a transfer of undulation between both yarns, occurring at each crossing point), and the second mechanism is the extension of the yarn, which occurs when the undulation transfer process has been exhausted (Fig. 6). The consideration of the yarn-yarn interactions leads to a stiffer response of the yarn (Fig. 6). In fact, during traction, the transverse yarns resists the yarn-yarn undulation transfer by increasing the reaction force. This explains why, without yarn-yarn interactions, the loss of undulation's process is more rapid compared to the case with yarn-yarn interactions.

5. Conclusion

We have developed a discrete mass-spring model of the mesoscopic mechanical behavior of a woven structure, taking into account the yarn compressibility and the yarn-yarn interactions at the mesoscopic scale. The focus has been on the more simple case of a single yarn interacting with the set of transverse yarns at the summit of its undulations. The stiffening effect of the yarn-yarn interactions on the fabric mechanical behavior has been evidenced. From our point of view, the main advantages of such a discrete approach are two fold:

(i) The interactions between yarns are modeled in a simple manner, without the need for a refined contact analysis;
(ii) It allows to separate and quantify the contributions of the flexional displacement (due to the undulations variation) and the contribution of the extensional displacement (due to the yarns stretching) during the fabric extension process.

The impact of the yarn interactions for the whole fabric under uniaxial and biaxial loading conditions shall further be investigated.

References

1. L. GAN, N. G. LY and G. P. STEEVEN, *Text. Res. J.* **65** (1995) 11.
2. J. W. EISCHEN, S. DENG and T. GLAPP, IEEE Computer graphics and Applications, 1996.
3. Y. F. ZHAO, T. N. WONG, S. T. TAN and W. J. CHEN, *Computer & Structures*, **63** (1997) 1.
4. P. BOISSE, M. BORR, K. BUET and A. CHEROUAT, *Composites Part B* **28B** (1997).
5. P. BOISSE, A. GASSER and G. HIVET, *Composites Part A* **32** (2001).
6. T. ISHIKAWA and T. CHOU, *J. Comp. Mater.* **17** (1983).

7. E. H. GLAESSGEN, C. M. PASTORE, O. H. GRIFFIN and A. BIRGER, *Comp. Part B* **27** (1996).
8. P. BOISSE, J. L. DANIEL, A. GASSER, G. HIVET and D. SOULAT, *Mec. Ind.* **1** (2001).
9. A. GASSER, P. BOISSE and S. HANKLAR, *Comp. Mater. Sci*. **17** (2000) 1.
10. H. HING and R. L. GRIMSDALE, *IEEE Computer Graphics and Applications* **16** (1996) 5.
11. B. BEN BOUBAKER, B. HAUSSY and J. F. GANGHOFFER, CRAS, *Série Mécanique* **330** (2002).
12. X. PROVOT, Graphics Interface, 1995.
13. J. PAGE and J. WANG, *Finite Element in Analysis and Design* **38** (2002) 8.
14. S. TIMOSHENKO, in "Théorie de la Stabilité Elastique" (Paris & Liège: Beranger, 1947) p. 21.
15. S. KAWABATA, M. NIWA and H. KAWAI, *Journal of the Textile Instituate* **64** (1973) 21.
16. P. BOISSE and M. BORR, *C. R. Acad. Sci. Paris, Série II b* **323** (1996).
17. P. BOISSE, K. BUET, A. GASSER and J. LAUNAY, *Composites Science and Technology* **61** (2001).
18. SNECMA Moteurs. Le Haillan, France. Internal Report, 2002.

Received December 2004
and accepted April 2005